Spring 5-2021

Modulation and Long-term Release of Cardiac Fibroblast Secretome to Enhance Cardiac Cell Survival under Hypoxia

JIN ZHAI
Washington University in St. Louis

Washington University in St. Louis

McKelvey School of Engineering

Department of Biomedical Engineering

Thesis Examination Committee:

Jianjun Guan

Dennis Barbour

Nathaniel Huebsch

Modulation and Long-term Release of Cardiac Fibroblast Secretome to Enhance Cardiac Cell Survival under Hypoxia

By

Jin Zhai

A thesis presented to the McKelvey School of Engineering of Washington University in St. Louis in partial fulfillment of the requirements for the degree of Master of Science

May 2021

St. Louis, Missouri

Dedicated to my parents.

Table of Contents

List of Tables

List of Figures

Acknowledgements

I would like to express my sincere thanks to my research advisor Dr. Jianjun Guan. Without his introduction and suggestion, I can't have the precious opportunity to join in the lab and do the project. I'd like to specially thank Ya Guan for helping me and giving me many suggestions and advice during the project. I'd like to thank the members in the lab. It is your effort that help me to achieve goals.

I'd like to thank my mother Huiling Lu and my father Guiyuan Zhai. Only with your support can I persist on pursuing my dreams.

Jin Zhai

Washington University in St. Louis

May 2021

Abstract

Modulation and Long-term Release of Cardiac Fibroblast Secretome to Enhance Cardiac Cell Survival under Hypoxia

By

Jin Zhai

Master of Science in Biomedical Engineering

Washington University in St. Louis, 2021

Professor Jianjun Guan

The irreversible damage to the heart caused by myocardial infarction (MI) leads to over one million deaths in the United States every year. There are several approaches to treat MI, such as angioplasty, redirected blood flow, and electrical medical devices, but they cannot promote new cardiac tissue generation, thus leading to potential high risk of re-surgeries. To overcome this limitation, stem cell therapy is regarded as a promising method. However, the implantation of stem cells has ethical and safe concern and the efficiency is limited due to low cell engraftment. Moreover, the effect of stem cell is predominantly attributed to paracrine effect. Therefore, the delivery of stem cell secretome is expected to be a prominent approach, since it has potential to achieve similar effect without causing safety and ethical problems with cell implantation. Among different cells, cardiac fibroblast (CF) is the largest cell population in the heart, and its secretome has been shown to protect cardiomyocytes under hypoxia. Thus, the objective of this work is to deliver CF secretome to the heart after MI. In the first part of this thesis, CF secretome was optimized in vitro by adjusting environmental oxygen condition and substrate stiffness. We found that the secretome collected under hypoxic condition (1% O_2) and soft substrate (6 kPa) can most effectively boost the survival of endothelial cells and cardiomyocytes under hypoxia. In the second

part, we developed platelet-membrane coated nanoparticles as a delivery vehicle for CF secretome. The nanoparticles had the capability of sustainedly releasing various growth factors such as PDGF, VEGF and bFGF. This secretome delivery system has potential to promote cardiac repair after MI.

Chapter 1 Introduction

1.1 Myocardial infarction

Myocardial infarction (MI) is the one of main causes of death worldwide. Over one million deaths due to MI are reported in the United State every year [1]. MI causes irreversible damage to the heart because of decreasing blood flow and lack of oxygen supply [2]. Currently, there are several kinds of treatment for MI. Patients can directly take drugs to break up blood clot or dissolve arterial blockage, such as aspirin and tissue plasminogen activator [2]. Also, some drugs can be injected in the blood to treat. Moreover, the angioplasty can be performed to open narrowed blood vessel and let blood flow easily [3]. To redirect blood flow around the blocked blood vessels, the coronary bypass surgery may be performed [4]. Furthermore, some electronic medical devices, such as pacemakers, can be implanted in the infarcted heart to keep regular beat [2]. For patients with end-stage heart failure, a heart transplantation may be required [2].

After MI, the loss of cardiomyocytes and formation of scar tissues are irreversible, leading to decreased cardiac function [5]. Thus, it is important to replace the injured cells. However, the existing surgical treatments are unable to promote the generation of new cardiac tissue. The application of stem cells can be a promising therapeutic option [6].

1.2 Stem cell therapy to treat MI

The use of stem cells to treat MI is expected by their two conspicuous capacities of self-renewal and differentiation into tissues [7]. In order to achieve the goal of regenerating the damaged tissues, the stem cell should be able to differentiate into cardiac lineages, such as myocytes and vascular endothelial cells [6]. The primary types of stem cells used in treatments for myocardial infarction are embryonic stem cells (ESCs), induced pluripotent stem cells (iPSCs), bone marrow mononuclear cells (BMMNCs), and mesenchymal stem cells (MSCs) [6]. Among

these stem cells, both ESCs and iPSCs are pluripotent and able to differentiate into all cell types, but ESCs may lead to ethical and safety concern, and iPSCs have the tumorigenic possibility [8,9]. BMMNCs has been shown to enhance left ventricular function, but they can differentiate into heterogeneous cell types which may not be advantaged for heart repair [6]. Although MSCs perform the immune-privileged ability , its cell retention, engraftment, and survival rate still is low [6].

Based on the above disadvantages of stem cell therapy, stem cell secretome has emerged as a promising therapeutic option. It has been shown that the key element of stem cell therapy should be attributed to its paracrine mechanism to promote regeneration [10].

1.3 Cell secretome

Stem cells can affect the surrounding cells by secreting soluble growth factors, cytokines, extracellular vesicles, and exosomes, altogether known as secretome [10]. As the part of composition of secretome, growth factors play a significant role in heart repair by promoting cell proliferation, cytoprotection, and migration. The commonly secreted factors include angiopoietin-1 (Ang-1), angiopoietin-2 (Ang-2), basic fibroblast growth factor (bFGF), platelet-derived growth factor (PDGF), vascular endothelial growth factor (VEGF), hepatocyte growth factor (HGF), tumor necrosis factor alpha (TNF-α), collagens, insulin-like growth factor 1 (IGF-1), interleukin-1 (IL-1), matrix metalloproteinases (MMPs), transforming growth factor beta (TGF-β), tissue inhibitor of metalloproteinases (TIMPs), bone morphogenetic protein 4 (BMP-4), interleukin-6 (IL-6), interleukin-7 (IL-7), neurotrophin-3 (NT-3), nerve growth factor (NGF), glial cell line-derive neurotrophic factor (GDNF), and brain-derived neurotrophic factor (BDNF). Among these factors, Ang-1, bFGF, IGF-1, IL-1, PDGF, VEGF, HGF, and TNF-α have been shown to be useful to angiogenesis in the heart [10]. Except for angiogenesis, bFGF, HGF, IGF-1,

IL-1, and VEGF also have been stated they have specific function in cardioprotection [10]. Moreover, several secreted factors can inhibit fibrosis, such as collagens, MMPs, TGF-β, and TIMPs [10].

1.4 Delivery system for cell secretome

In order to deliver secretome to the damaged tissues, several approaches have been investigated, such as transplantation of artificial cardiac patch encapsulated secreted factors from stem cells, injectable and biocompatible hydrogels as carriers of secretome, injectable nanofibers bonded with secretome, and biomimetic nanoparticles [11–15]. Huang et al. have developed therapeutic cardiac patch to deliver the secreted factors of cardiac stromal cells to rat/porcine heart after MI, and they found that the cardiac recovery was supported by reducing scarring and improving angiomyogenesis [11]. An injectable hydrogel has been developed by Waters et al to deliver secretome secreted by human adipose-derived stem cells to the peri-infarct myocardium, leading to decreased scar area and increased cardiac function [12]. Webber et al. have designed a factor-loaded injectable nanofiber network and injected into mouse heart after MI, and the preservation of haemodynamic function was found by them [13]. Yasin et al have fabricated nanoparticles loaded with VEGF to a murine myocardial infarction model, followed by reductions infarct size and angiogenesis [16].

Chapter 2 Modulation of Cardiac Fibroblast Secretome in Response to Different Environmental Cues

2.1 Introduction

Compared to the disadvantages of stem cells, which are the unlimited cell types differentiated from stem cells, the sophisticated extraction procedure, and high cost, the advantage of cardiac fibroblasts (CFs) is prominent. CFs has been defined as the main effector to prevent heart rupture by secreting factors in the infarcted heart [17]. Moreover, the large number of CFs is easier to obtain compared to stem cells. Furthermore, the largest cell numbers in the heart are cardiac fibroblasts, which has been shown to be conductive to mechanical, structural, and biochemical properties of the heart [18]. Compared to other stem cells, CFs are the host cells obtained the natural advantages. CFs also have been stated to be able to secrete a large number of growth factors used in treatments for MI, such as VEGF, PDGF, bFGF, TNF-α, and IL-1β [19]. Furthermore, the secreted factors from CFs can protect cardiomyocytes from hypoxic condition, induced hypertrophy, and ischemia injury [20].

2.2 Materials and methods

2.2.1 Materials

Acrylamide and N,N′-methylenebisacrylamide were purchased from Sigma-Aldrich. N,N,N′,N′-Tetramethylethylenediamine (TEMED) and ammonium persulfate (APS) were purchased from Bio-rad. Isopropanol was purchased form Fisher Scientific. Collagen type I was obtained from Corning. Hydrophobic glass slides were purchased from Bio-rad. TRI Reagent was purchased from Sigma. Acid phenol:$CHCl_3$ was purchased from Ambion. Nuclease-free water and SYBR Green were purchased from Thermo Scientific. High-capacity cDNA reverse transcription kit was purchased from Thermo Fisher Scientific.

2.2.2 RCF culture

Rat cardiac fibroblasts (RCFs) were cultured and seeded in a T75 flask with 10 mL culture medium consisting of Dulbecco's modified Eagle medium (DMEM), 12% fetal bovine serum (FBS), and 1% penicillin/streptomycin under normal culture conditions (21% O_2, 5% CO_2, 37°C). The culture medium was changed every two days and RCFs were passaged when 90% confluency was reached.

After 90% confluency was reached, RCFs were digested using 0.25% trypsin/EDTA for 5 mins at 37℃ and centrifuged at 1600 rpm for 7 min. Collected cells were seeded in 100-mm dishes supplemented with culture medium consisting of DMEM, 12% FBS, and 1% penicillin. The cells were maintained under normal culture conditions (21% O_2, 5% CO_2, 37°C) overnight. The medium was then replaced with serum-free medium. One dish was incubated under hypoxic condition (1% O_2, 5% CO_2, 37°C) for 24 hours. One dish was incubated under 5% O_2 and 5% CO_2 at 37°C for 24 hours. One dish was incubated under normal culture condition (21% O_2, 5% CO_2, 37°C) for 24 hours. After incubation, the media was aspirated, and the cells were lysed using 1 mL of TRI reagent and then transferred into a 1.7 mL centrifuge tube to store at -80℃ for further experiments.

2.2.3 PAM gel fabrication and characterization

Acrylamide, bis-acrylamide, and APS were dissolved in deionized (DI) water to form solutions with concentration of 40% w/v, 2% w/v, and 10% w/v, respectively. Polyacrylamide (PAM) gel solution was prepared by mixing 40% w/v acrylamide solution, 2% w/v bis-acrylamide solution, and DI water at 4 different ratios [21]. The ratio of these reagents and the abbreviation of the corresponding gel were specified in **Table 1**. 5mL of polyacrylamide gel solution was placed into a 50-mL tube. 25 μL of 10% w/v APS and 2.5 μL of TEMED were

added into the same tube to achieve final concentration of 0.05% and 0.5%, respectively. The solution was gently mixed by pipetting up and down 10 – 15 times. The gel solution was pipetted onto the 0.75 mm space which was hold by two hydrophobic glass slides. 500 µL of isopropanol was pipetted above the gel solution to remove bubbles. After 1 hour, the PAM gel was peeled off carefully. To obtain a desired shape which was similar to the plate well of a 6-well plate, the cap of a 50-mL tube was used to cut PAM gels to circles. One PAM gel was placed in each well by forceps.

To determine PAM gels stiffness, the storage modulus was measured by rheometer. The Young's modulus, E was related to storage modulus by using the equation: $E = G'2(1 + v)$, where v, the Poisson ratio was approximated to 0.5 for PAM gel [22].

2.2.4 Collagen coating of PAM gels

Before coating, the 6-well plate was placed under an UV lamp for 1 hour while all PAM gels were soaked in 1x phosphate buffered saline (PBS) to keep hydrated. 0.2 mg/mL collagen solution was prepared by diluting the 3.78 mg/mL collagen type I solution in PBS. 500 µL of diluted collagen solution was pipetted into each well to completely cover the gel surface. The plate was covered by parafilm and placed at 4℃ overnight to allow collagen coating. After aspirating collagen solution and rinsing with PBS to remove excess collagen solution, the plate was placed in a biosafety cabinet under UV to sterilize for 1 hour.

2.2.5 Immunocytochemical staining

RCFs were cultured and seeded on PAM gels in 6-well plate with 2 mL culture medium consisting of DMEM without serum at a hypoxia incubator (1% O_2, 5%CO_2, 37°C) overnight. RCFs were fixed with 500 µL of 4% paraformaldehyde (PFA) solution. After fixation for 50 mins, blocking buffer was added to each well and incubated for 1 hour. Then, the fixed cells

were incubated with mouse anti-alpha smooth actin-alpha (α-SMA, Abcam) at 4 C overnight. Goat anti-mouse Alexa Fluor 647 (Invitrogen) was used as a secondary antibody to stain the cells at room temperature for 1 hour. Nuclei and cytoplasm were stained with DAPI (Sigma) and F-actin (Invitrogen), respectively. Fluorescent images were taken using a confocal microscope (Olympus FV1200).

2.2.6 RCF secretome collection

After 90% confluency was reached, RCFs were digested using 0.25% trypsin/EDTA for 5 mins at 37℃. Collected cells were seeded onto the PAM gels supplemented with culture medium consisting of DMEM, 12% FBS, and 1% penicillin. The cells were left to settle under normal culture conditions (21% O_2, 5% CO_2, 37°C) overnight. The medium was then replaced with serum-free medium, and the plate was incubated under hypoxic condition (1% O_2, 5% CO_2, 37 °C) for 24 hours. The medium of each PAM gel was collected, filtered by 0.22 μm filter, and stored at –80°C for further experiments. The secretomes collected on 4 PAM gels with different stiffness were named as PAM1, PAM2, PAM3, PAM4, respectively. The remaining cells were collected for mRNA collection.

2.2.7 mRNA collection and concentration measurement

Cells from RCF secretome collection were lysed using 1 mL of TRI reagent and then transferred into a 1.7 mL centrifuge tube to incubate at room temperature for 5 mins. 150 μL phenol/$CHCl_3$ was added to mixture until it became cloudy. The tube was vortexed for 20 seconds and then incubated at room temperature for 10 mins, followed by centrifugation at 12,000 g, 4℃ for 15 mins. After centrifugation, the upper transparent RNA-rich layer was collected in a new 1.7 mL centrifuge tube, following by adding 150 μL isopropanol. The tube was vortexed for 20 seconds and then incubated at room temperature for 15 mins. The tube was

centrifuged at 12,000 g, 4°C for 10 mins. After centrifugation, the supernatant was removed, followed by adding 150 µL of 75% ethanol (in DEPC water). The tube was vortexed for 20 seconds and centrifuged at 12,000 g, 4°C for 5 mins. After centrifugation, the supernatant was removed. The open capped tube was placed in the biosafety cabinet for 20 mins to air-dry. 22 µL nuclease free water was added to dissolve the remaining RNA. RNA concentration was measured by NanoDrop (ND-1000 Spectrophotometer) for cDNA synthesis.

2.2.8 cDNA synthesis

Complementary DNA (cDNA) was synthesized at 1000 ng/reaction using a high capacity cDNA reverse transcription kit (Thermo Fisher) by Mastercycler (Eppendorf). The synthesized cDNA was stored at – 20°C for Real-time RT-PCR.

2.2.9 Real-time RT-PCR

As described at cDNA Synthesis, cDNA was obtained. SYBR green (Invitrogen) and selected primer pairs (Table 2) were mixed to perform real-time RT-PCR. β-actin was served as a housekeeping gene. Fold of increase was calculated using ΔΔCt method.

2.2.10 Sodium dodecyl sulphate–polyacrylamide gel electrophoresis (SDS-PAGE)

Protein concentration was measured using Bradford protein assay.

Mini-protean TGX stain-free precast gel (Bio-rad) was used to load proteins. 20 ug protein was loaded in each lane. The running buffer for SDS-PAGE was 25 mM Tris, 190 mM glycine and 0.1% SDS. The voltage was kept at 30 V for 15 min and 80 V for 1 hour. The images of the gel were obtained by Chemi-Doc XRS+ system (Bio-rad)

2.2.11 Enzyme-linked immunosorbent assay (ELISA)

100 μL diluted capture antibody was added to each well of a 96-well plate, followed by sealing with parafilm and incubating overnight at room temperature. The remaining liquid was aspirated, following by washing with wash buffer (0.05% Tween-20 in PBS) for 4 times. After that, 300 μL block buffer (1% bovine serum albumin in PBS) was added to each well and incubated for 1 hour at room temperature. Then, liquids were aspirated, and the plate was washed with wash buffer for 4 times. Serial diluted standard protein and release media were added to the plate with replicate number of 3, followed by incubating at 4℃ overnight. Then, the remaining liquid was aspirated, followed by washing with wash buffer for 4 times. Diluted detection antibody was added to each well and incubated for 2 hours at room temperature. After that, the liquids were aspirated and followed by washing with wash buffer for 4 times. Diluted Avidin-HRP conjugate was added to each well and incubated for 30 min at room temperature. Then, the liquids were aspirated and followed by washing with wash buffer for 4 times. ABTS liquid substrate solution was added to each well and incubated at room temperature in the dark. The color development was monitored by a plate reader at 405 nm with wavelength correction at 650 nm.

2.2.12 HUVEC culture

Human umbilical vein endothelial cells (HUVECs) were cultured and seeded in a T75 flask supplemented with 10 mL culture medium consisting of EBM and EGM-2 SingleQuots (Lonza) under normal culture conditions (21% O_2, 5% CO_2, 37°C). The culture medium was changed every two days and HUVECs were passaged when 90% confluence was reached.

2.2.13 HUVEC survival (MTT assay)

As previously described at RCF secretome collection, the medium of each PAM gel was collected. The medium of PAM2 and EBM without serum were blended at a ratio of 1:1 at a T25 flask, following by being incubated under hypoxic condition (1% O_2, 5% CO_2, 37°C) for over 24 hours to allow gas balance. The medium of PAM4 and EBM without serum were blended at a ratio of 1:1 at a T25 flask, following by being incubated under hypoxic condition (1% O_2, 5% CO_2, 37°C) for over 24 hours. All media used in this experiment was stored at hypoxic incubator (1% O_2, 5% CO_2, 37°C) for future experiments. Also, EBM without serum was placed to a T25 flask and incubated under hypoxic condition (1% O_2, 5%CO_2, 37 °C) for over 24 hours, named as Control medium stored at hypoxic incubator (1% O_2, 5% CO_2, 37°C) for further experiments.

HUVECs were cultured and seeded in two 96-well plates (concentration of 30,000 cells/mL) with replicate number of 10 for each group supplemented with 200 µL culture medium. The cells were maintained under normal culture conditions (21% O_2, 5% CO_2, 37°C) overnight. Without changing culture medium, two plates were transferred to hypoxic incubator (1% O_2, 5% CO_2, 37°C) and incubated. At day 0 and day 4, cell viability was measured for control group, PAM2 group (secretome collected on PAM2 gel blended with EBM) and PAM4 group (secretome collected on PAM4 gel blended with EBM) using MTT assay. Briefly, 20 µL 5 mg/mL MTT solution was added to each well to incubate for 4 hours. After that, the medium was removed carefully and 200 µL DMSO was added to each well, following by shaking for 10 mins to dissolve all solids at bottom and reading the absorbance at 560 nm by a plate reader, and substracting background at 670 nm.

2.2.14 HUVEC migration

HUVECs were cultured and seeded in a 24-well plate (concentration of 175,000 cells/mL) with replicate number of 4 for each group supplemented with 800 µL culture medium. The cells were left to settle under normal culture conditions (21% O_2, 5% CO_2, 37°C). After ~90% confluency was reached, the cell monolayer was scratched using a pipette tip, and the cells were treated with EBM medium (control group) and secretome collected on PAM2 gel blended with EBM (PAM2 group). At 0, 15, 24, and 40 hours, cell migration was quantified by taking images with an optical microscope (Olympus IX70).

2.2.15 HUVEC tube formation

Three-dimensional collagen gel solution was prepared by mixing 3.78 mg/mL collagen type I solution, 5x DMEM, 1x DMEM, and FBS and adjusting pH to 7.3 by adding 1 M NaOH, followed by pipetting up and down 10 times. 500 µL solution was added to each well of a 48-well plate with replicate number of 2 for each group. After 1-hour incubation, the remaining liquid was aspirated, following by washing with PBS for 2 times.

HUVECs were seeded in collagen gels (concentration of 50,000 cells/mL) supplemented with 400 µL culture medium. The cells were left to settle under normal culture conditions (21% O_2, 5% CO_2, 37°C) for 24 hours. The cells were treated with EBM medium (control group) and secretome collected on PAM2 gel blended with EBM (PAM2 group). After 24-hour incubation, the medium was aspirated, following by washing with PBS. HUVECs were fixed using 4% PFA for 50 min, followed by washing with PBS for 4 times. After that, cells were blocked using blocking buffer for 40 min, followed by washing with PBS. The diluted F-actin and DAPI were used to stain cells for 1 hour, followed by washing with PBS for 5 times. Fluorescent images

were taken for each collagen gel using Olympus FV1200 confocal microscope. The tube density was quantified from large lumens.

2.2.16 Cardiomyocyte culture

Rat neonatal cardiomyocytes were purchased from Lonza and cultured per manufacturer's instruction. Briefly, the cells were seeded in nitrocellulose-coated plates with rat cardiomyocyte growth media (rCGM, Lonza). Bromodeoxyuridine was added to the culture media to suppress fibroblast formation.

2.2.17 Cardiomyocyte survival (MTT assay)

Cardiomyocytes were seeded in two 96-well plates (concentration of 10,000 cells/mL) with replicate number of 5 for each group supplemented with 200 μL culture medium. At day 0 and day 2, cell viability was measured for control group, PAM2 group (secretome collected on PAM2 gel blended with EBM) and PAM4 group (secretome collected on PAM4 gel blended with EBM) using MTT assay. Briefly, 20 μL 5 mg/mL MTT solution was added to each well to incubate for 4 hours. After that, the medium was removed carefully and 200 μL DMSO was added to each well, following by shaking for 10 mins to dissolve all solids at bottom and reading the absorbance at 560 nm by a plate reader, and substracting background at 670 nm.

2.2.18 Statistical analysis

All data were presented as mean ± standard deviation. One-way ANOVA was used to analyze the significant difference between experimental groups. The significant difference was defined as $p < 0.05$.

2.3 Results and Discussion

2.3.1 Gene expression of RCF secretome in response to oxygen content

To investigate how the RCF secretome changed in response to environmental oxygen content, the growth factor expressions were quantified at the mRNA level under 1% O_2, 5% O_2, and 21% O_2 culture conditions. RCF secretome under 1% O_2 exhibited significantly higher Vascular endothelial growth factor (VEGF) expression than 5% O_2 ($p<0.0001$) and 21% O_2 ($p<0.0001$) (Figure 1a). Besides VEGF, the 1% O_2 group had significantly lower interleukin (IL1β) expression ($p<0.05$) and transforming growth factor β (TGFβ) expression ($p<0.001$) than 21% O_2, whereas 1% O_2 and 5% O_2 had similar expressions ($p>0.05$) (Figure 1b, 1c).

VEGF is one of the most effective proangiogenic factors [23]. It also plays a crucial role in promoting the formation of new blood vessels in the heart with myocardial infarction or other ischemic heart diseases [16]. Thus, the significantly higher VEGF expression was the advantage of 1% O_2 group compared to other groups. Moreover, suppression of IL1β has been proven to be a treatment in myocardial infarction [24]. It has been shown that the expression of genes which are essential to the regulation of calcium homeostasis are reduced by IL1β [25]. The expression of nitric oxide synthase in cardiac myocytes is promoted by IL1β [26]. In addition, TGFβ has been proven to induce myocardial infarction and activate fibrosis in the infarcted heart [27]. Therefore, the lower expression of IL1β and TGFβ was another advantage of 1% O_2 group compared to other groups. The above results reveal that the lower environmental oxygen content significantly optimized RCF secretome. Hypoxic culture condition (1% O_2, 5% CO_2, 37°C) was chosen for further experiments.

2.3.2 PAM Gel Fabrication and Characterization

PAM gels were fabricated with four different concentrations of acrylamide and crosslinker bis-acrylamide and cut to circles (Figure 2a). To determine PAM gels stiffness, the storage modulus was measured by using rheometer (Table 3). The Young's modulus, E was related to storage modulus by using the equation: $E = G'2(1 + v)$, where v, the Passion ratio was approximated to 0.5 for PAM gels [22]. For PAM1 which contained 5% acrylamide and 0.1% crosslinker bis-acrylamide, its storage modulus was 0.43 ± 0.02 kPa and Young's modulus was 1.29 ± 0.05 kPa. For PAM2 which contained 8% acrylamide and 0.1% crosslinker bis-acrylamide, its storage modulus was 2.04 ± 0.10 kPa and Young's modulus was 6.11 ± 0.31 kPa. For PAM3 which contained 8% acrylamide and 0.25% crosslinker bis-acrylamide, its storage modulus was 4.82 ± 0.09 kPa and Young's modulus was 14.46 ± 0.27 kPa. For PAM4 which contained 12% acrylamide and 0.25% crosslinker bis-acrylamide, its storage modulus was 10.83 ± 0.10 kPa and Young's modulus was 32.50 ± 0.31 kPa (Figure 2b). These results confirmed that the stiffness of PAM gel was controllable by adjusting the concentration of acrylamide or crosslinker (bisacrylamide) concentration. We found that higher acrylamide or crosslinker (bisacrylamide) concentration resulted in stiffer PAM gel.

To determine RCF morphology and the tendency to differentiate into myofibroblasts, immunocytochemical staining of SMA was performed, and the fluorescent images were taken for RCF on PAM1 to 4 and normal culture plate (Figure 3). α-SMA is regarded as a marker for myofibroblasts [28]. With the increase of stiffness, the α-SMA expression increased and the RCFs were observed to differentiate into myofibroblasts. The above results demonstrate that the stiffness of PAM gel could affect the α-SMA expression. Higher stiffness of PAM gel could lead to more α-SMA expression. RCFs would differentiate into myofibroblasts on a stiffer substrate.

Fibroblasts has been shown to proliferate, migrate, and regulate cardiac extracellular matrix (ECM), leading to sustain cardiac homeostasis [29]. Myofibroblasts are differentiated from fibroblasts, which are unusually present in the healthy myocardium, but normal in the infract scar, leading to fibrogenesis [30]. The activeness of myofibroblasts in healthy area of the heart can lead to fibrosis and adverse myocardial remodeling [31]. Myocardial remodeling (REM) is a detrimental process of changing in the heart's size and shape, being caused by myocardial infarction [32]. High myofibroblast density in the remote myocardium results in increased myocardial stiffness, leading to systolic and diastolic dysfunction and heart failure [29]. Moreover, compared to the proven myocyte hypertrophy caused by secretome activated myofibroblasts, secretome of CFs has been performed to protect cardiomyocytes from induced hypertrophy [20,33]. Therefore, the PAM gel with less α-SMA expression performed greater than others.

2.3.3 Effects of PAM gels on RCF secretome under hypoxic condition

To investigate how the stiffness of PAM gels affects RCF secretome under hypoxic condition, the total amounts of protein in RCF cultured on PAM1 to 4 were measured by running SDS-PAGE (Figure 4). Compared to other three groups, the PAM2 groups expressed apparently much greater amount of protein.

To determine how RCF paracrine effects were expressed on PAM gels under hypoxic condition, the growth factor expressions were quantified at the RNA level. For basic fibroblast growth factor (bFGF), the PAM2 group exhibited significantly higher than PAM3 group ($p<0.05$) and PAM4 group (0.01) (Figure 5a). For platelet-derived growth factor (PDGF), the PAM2 group also performed significantly higher than PAM3 group ($p<0.01$) and PAM4 group

($p<0.0001$) (Figure 5b). For VEGF, the PAM2 group also performed significantly higher than PAM3 group ($p<0.05$) (Figure 5c).

bFGF has been shown to be a protective role in myocardial infarction and hypoxia cardiomyocytes [34]. Also, bFGF can promote cardiac stem cell migration, reduce infarct size, and enhance cardiac systolic function [35,36]. Moreover, it has been shown that PDGF is one of the growth factors which can promote cell growth, differentiation, proliferation, and migration, leading to stimulate angiogenesis [37]. The importance of VEGF in myocardial infarction has been discussed before. Thus, the significantly higher expressions of PDGF, VEGF, and bFGF were the advantage of PAM2 group compared to other three groups. The above results demonstrate that PAM2 gel optimized RCF secretome under hypoxic condition.

To determine the concentration of bFGF of RCF secretome collected on PAM1 to 3 under hypoxia, ELISA was used to measure. The PAM2 gel significantly increased the concentration of bFGF in RCF secretome compared to PAM1 ($p<0.01$) and PAM3 ($p<0.01$) (Figure 6). These results demonstrate that PAM2 significantly enhanced the amount of bFGF in RCF secretome under hypoxia.

Therefore, based on the above results, PAM2 group was chosen for further experiments.

2.3.4 Effects of RCF secretome on HUVEC survival, migration and tube formation under hypoxic condition

Endothelial cells play a pivotal role in angiogenesis, which is a crucial process after myocardial infarction. The survival, migration and fusion of endothelial cells is the prerequisite for formation of new blood vessels [38].

To investigate whether the PAM2 can increase HUVEC survival under hypoxic condition, HUVECs were cultured using three different culture media. Control group was used with serum-free medium; PAM2 group was used with serum-free medium and PAM2 medium at ratio of 1:1; PAM4 group was used with serum-free medium and PAM4 medium at ratio of 1:1. Although the cell viability of all three groups at day 4 decreased compared to day 0, the cell number of PAM2 group was significantly higher than control group ($p<0.0001$) and PAM4 group ($p<0.01$) (Figure 7). Moreover, there was no significant difference between control group and PAM4 group ($p>0.05$). The in vitro results reveal that the secretome collected on low stiffness promoted HUVEC survival under hypoxic condition, but the secretome collected on high stiffness did not have much greater effect than serum-free medium. Thus, PAM2 medium was used for further experiment.

To determine whether the RCF secretome collected on PAM2 enhanced HUVEC migration, the migration ratio of two groups (Control and PAM2) was statistically measured based on images taken at 0, 15, 24, and 40 hours (Figure 8a). For control group, the migration ratios at 15, 24, and 40 hours were lower than 20%. For PAM2 group, the migration ratios at 15, 24, and 40 hours were persistently increasing. At these three time spots, PAM2 group had significantly greater migration ratios than control group ($p<0.0001$) (Figure 8b).

To investigate whether the RCF secretome collected on PAM2 promoted HUVEC tube formation, the normalized tube density of two groups was statistically measured based on fluorescent images taken after 24-hour incubation (Figure 9a). For the number of cells, PAM2 group performed apparently much greater than control group. Besides the number of cells, PAM2 group had significantly greater tube density than control group ($p<0.001$) (Figure 9b).

The above results reveal that the RCF secretome collected on PAM2 played an essential role on HUVEC survival, migration, and tube formation.

2.3.5 Effect of RCF secretome on cardiomyocytes survival under hypoxic condition

To investigate whether the PAM2 can increase cardiomyocytes survival under hypoxic condition, cardiomyocytes were cultured using three different culture media. Control group was used with serum-free medium; PAM2 group was used with serum-free medium and PAM2 medium at ratio of 1:1; PAM4 group was used with serum-free medium and PAM4 medium at ratio of 1:1. Although the cell viability of all three groups at day 2 decreased compared to day 0, the cell number of PAM2 group were significantly higher than control group ($p<0.01$) and PAM4 group ($p<0.001$) (Figure 10). Moreover, there was no significant difference between control group and PAM4 group ($p>0.05$). The in vitro results reveal that the secretome collected on low stiffness protected cardiomyocytes under hypoxic condition, but the secretome collected on high stiffness did not have greater effect than serum-free medium.

2.4 Conclusion

In this work, RCF secretome was modulated in response to different environmental oxygen contents and stiffness. Under hypoxic culture condition (1% O_2, 5% CO_2, 37°C), the RCF secretome collected on PAM2 gel exhibited greater secretion of growth factors cytokines at both RNA and protein level. Higher cell survival ratio, migration ratio, and tube formation ratio confirmed the useful treatment of optimized RCF secretome. This modulation of cardiac fibroblast secretome may promote heart repair after myocardial infarction.

Chapter 3 Targeted Delivery of Platelet Membrane Coated PLGA Nanoparticles with Sustained Cardiac Fibroblast Secretome Release

3.1 Intro

Among the current delivery methods, such as injectable hydrogel and transplantation of patch, they are limited by indirect delivery with a surgery to open chest, leading to high risk to break myocardium [39]. In addition, nanoparticle delivery system is a minimally-invasive method by intravenous injection, and its size is small enough to circulate in the blood stream [40]. To overcome the limitations of nanoparticle, such as short retention and potential immune rejection, a cell-membrane coated nanoparticle delivery system has been designed [41]. Among various cell membranes, platelet membrane coating has advantage of avoiding immune rejection, capability of ligand binding and selectively binding to injured endothelium by nature. The objective of this work is to coat platelet membrane with nanoparticles to targeted bind to the injured endothelium [42].

3.2 Materials and methods

3.2.1 Materials

Poly (lactide-co-glycolic acid) (PLGA, LACTEL) with a LA/GA ratio of 50/50 was purchased from Lactel Absorbable Polymers.

3.2.2 Secretome collection

As described at RCF secretome collection, the medium of PAM2 was collected, filtered by 0.22 μm filter, and freeze-dried. The powder was dissolved in 2 mL DI water, and concentrated using vivaspin 500 concentrator (MWCO=3kDa) to obtain a desalted secretome solution for nanoparticle fabrication.

3.2.3 Nanoparticle fabrication and characterization

100 mg PLGA was weighed and dissolved in 2 mL dichloromethane (DCM). 200 μL secretome solution was emulsified with PLGA solution using an ultrasonicator for 1 min to obtain a homogeneous and opaque solution. The solution was quickly transferred into a beaker with 8 mL of 1% w/v polyvinyl alcohol (PVA) water solution, following by 1-minute ultrasonication. After that, the beaker was placed on a magnetic stirring plate with a moderate stirring speed at room temperature overnight to evaporate solvent. The remaining solution was transferred into a 50-mL tube, following by adding DI water to 35 mL and centrifuging at speed of 12,000 rpm for 15 mins. After centrifugation, the supernatant was removed carefully. The centrifugation/resuspension process was repeated for 4 times to remove PVA. After that, the washed nanoparticles were freeze-dried, collected, and stored at -80℃ for further experiments.

The size distribution of nanoparticles was measured by dynamic light scattering at room temperature. The samples were prepared by diluting nanoparticles with DI water and filtering with a 0.45 μm membrane filter.

3.2.4 Growth factor release characterization

75 mg of fabricated nanoparticles was weighed and suspended in 5 mL PBS with 1% penicillin to achieve a final concentration of 15 mg/mL. The suspension was evenly separated into twelve 1.7-mL centrifuge tube and incubated in a 37℃ water bath for release. At day 1, 2, 3, 5, 7, 10, and 14, the release media were collected and stored at -80℃ for further experiments.

The concentration of growth factor was measured by ELISA [43,44]. 100 μL diluted capture antibody was added to each well of a 96-well plate, followed by sealing with parafilm and incubating overnight at room temperature. The remaining liquid was aspirated, followed by washing with wash buffer (0.05% Tween-20 in PBS) for 4 times. After that, 300 μL block buffer

(1% Bovine Serum Albumin in PBS) was added to each well and incubated for 1 hour at room temperature. Then, liquids were aspirated, and the plate was washed with wash buffer for 4 times. Serial diluted standard and release media were added to the plate with replicate number of 3, followed by incubating at 4℃ overnight. Then, the remaining liquid was aspirated, followed by washing with wash buffer for 4 times. Diluted detection antibody was added to each well and incubated for 2 hours at room temperature. After that, the liquids were aspirated and followed by washing with wash buffer for 4 times. Diluted Avidin-HRP conjugate was added to each well and incubated for 30 mins at room temperature. Then, the liquids were aspirated and followed by washing with wash buffer for 4 times. ABTS liquid substrate solution was added to each well and incubated at room temperature in the dark. The color development was monitored by a plate reader at 405 nm with wavelength correction set at 650 nm.

3.2.5 Platelet membrane coating and characterization

The platelet rich plasma was extracted from bovine blood. Three freeze-thaw processes were conducted on the platelets in a 1.7-mL centrifuge tube to break the cell membrane. After the final thaw process, the tube was centrifuged at 4,500 g for 5 min at room temperature. Then, the pelleted platelet membrane was washed with PBS containing protease inhibitor for 3 times. After sonication for 5 min, 2 mg freeze-dried nanoparticles were added into 2 mL platelet membrane solution, following by sonicating for 5 mins. The platelet membrane coated (PLM-coated) nanoparticles were stored at 4℃ for further experiments.

The size distribution of platelet membrane coated nanoparticles was measured by dynamic light scattering at room temperature. The samples were prepared by diluting nanoparticles with DI water and filtering with a 0.45 μm membrane filter.

3.2.6 Cell uptake

As described at Platelet membrane coating and characterization, PLM-coated nanoparticles were obtained. Ischemia-targeting peptide CSTSMLKAC (CST) in NaH_2PO_4 buffer was mixed with PLM-coated nanoparticles, following by adding suberic acid bis(N-hydroxysuccinimide ester) dissolved in DMSO and stirring at room temperature for 2 hours. After adding glycine and dialyzing against DI water overnight, CST conjugation was finished.

Glass slides were placed in a 24-well plate, coated with collagen, and incubated for 1 hour at room temperature. After the remaining liquids were aspirated, the plate was placed in a biosafety cabinet under UV to sterilize for 1 hour. HUVECs and RCFs were cultured and seeded in the glass slides (concentration of 50000 cells/mL) with replicate number of 2 for each kind of cells supplemented with 800 μL culture medium. The cells were left to settle under normal culture conditions (21% O_2, 5% CO_2, 37°C). After 24-hour incubation, the medium was replaced with 1 mg/mL diluted, conjugated PLM-coated nanoparticles with normal medium. After 24-hour incubation, the medium was aspirated, following by washing with PBS. HUVECs and RCFs were fixed using 4% PFA for 50 mins, following by washing with PBS for 4 times. After that, cells were blocked using blocking buffer for 40 mins, following by washing with PBS. The diluted F-actin and DAPI were used to stain cells for 1 hour, following by washing with PBS for 5 times. Fluorescent images were taken for each glass slide using Olympus FV1200 confocal microscope. The ratios of cell uptake were quantified by measuring the number of cells which have nanoparticles inside divided by total number of cells.

3.2.6 Statistical analysis

All data were presented as mean ± standard deviation. One-way ANOVA was used to analyze the significant difference between experimental groups. The significant difference was defined as $p < 0.05$.

3.3 Results and Discussion

3.3.1 Fabrication and characterization of PLGA nanoparticles

The PLGA nanoparticles were fabricated by the method of double emulsion to form core-shell structure with PLGA as shell and RCF secretome as core. The size of uncoated PLGA nanoparticles was 218.33 nm with a PDI of 0.17, while the size of PLM-coated PLGA nanoparticles was 239.80 with a PDI of 0.04 (Figure 11a). The results demonstrate that the size of nanoparticles increased after coating with platelet membrane (Table 3). The size of PLGA nanoparticles did not change significantly within 30-day incubation in PBS at 37ºC (Figure 11b). The above results reveal that the PLGA nanoparticles were stable in physiological environment.

3.3.2 Growth factor release kinetics

To determine how different growth factors released from the nanoparticles, the concentrations of PDGF, VEGF, and bFGF in release media were measured and calculated by performing ELISA (Figure 12). The above results demonstrate that the growth factors were sustainedly released by nanoparticles in 37°C over 14 days.

Herein, among PDGF, VEGF, and bFGF, they all play essential roles in the treatment of myocardial infarction. The sustained release delivery system is useful to avoid a consequence that the loaded secretome are metabolized and eliminated from the body too fast to achieve the desired therapeutic effect [45].

3.3.3 Cell uptake for platelet membrane coated nanoparticles

To investigate how the platelet membrane affected HUVEC and RCF uptake nanoparticle, the ratio of cell uptake was quantified by counting the number of cells endocytosed nanoparticles. For both of HUVEC and RCF, the ratios of cell uptake were lower than 15% (Figure 13).

3.4 Conclusion

In this work, a RCF secretome release system was designed and fabricated. The RCF secretome nanoparticles exhibited sustainedly release RCF secretome and stability in physiological environment. This delivery system may have the potential treatment for the heart repair following myocardial infarction.

Chapter 4 Future Work

The PLM-coated PLGA nanoparticles can sustainedly release the loaded RCF secretome which is modulated based on hypoxic culture condition and environmental stiffness. However, we still do not know whether the amount of secretome loaded is enough to promote heart repair following myocardial infarction. The effect of secretome loaded nanoparticles should be tested by further and deeper experiments in vitro and in vivo. Thus, the therapeutic effect of this nanoparticles can be exhibited.

Table 1. Concentration of acrylamide and bis-acrylamide of PAM gels.

Polyacrylamide hydrogel	Acrylamide %	Bis-acrylamide %	Acrylamide from 40% stock solution (mL)	Bis-acrylamide from 2% stock solution (mL)	DI water (mL)
PAM1	5	0.1	0.625	0.25	4.125
PAM2	8	0.1	1	0.25	3.75
PAM3	8	0.25	1	0.625	3.375
PAM4	12	0.25	1.5	0.625	2.875

Table 2. Primer sequences used in real-time RT-PCR.

	Forward primer	Reverse primer
VEGF	TATCTTCAAGCCGTCCTGTG	GATCCGCATGATCTGCATAG
PDGFBB	AAATCGTGGAAGACATGAAC	TTCACAAGCACAATGCAC
TGFβ	ATATAGCAACAATTCCTGGC	CGTGGAGTACATTATCTTTGC
bFGF	AACTACAGCTCCAAGCAG	GTAACACACTTAGAACCAG
IL1β	CACCTCTCAAGCAGAGCACAG	GGGTTCCATGGTGAAGTCAAC

Table 3. PAM gel stiffness measured by rheology.

Polyacrylamide hydrogel	**Storage Modulus G' ± SD (kPa)**	**Young's Modulus E ± SD (kPa)**
PAM1	0.43 ± 0.02	1.29 ± 0.05
PAM2	2.04 ± 0.10	6.11 ± 0.31
PAM3	4.82 ± 0.09	14.46 ± 0.27
PAM4	10.83 ± 0.10	32.50 ± 0.31

Table 4. Size and PDI of uncoated and PLM-coated nanoparticles.

	Z-average (nm)	**PDI**
Uncoated nanoparticle	218.33	0.17
PLM-coated nanoparticle	239.80	0.04

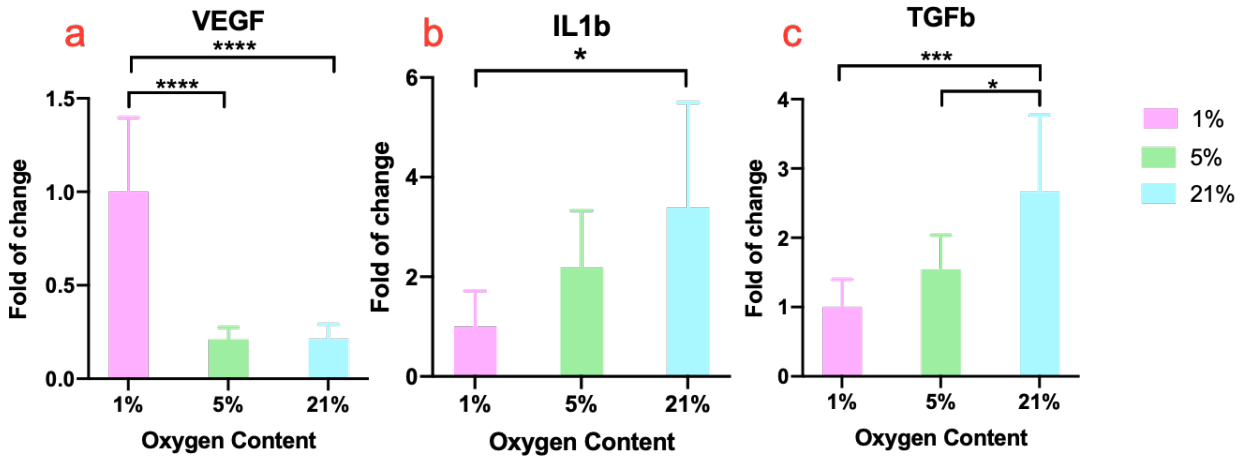

Figure 1. Gene expression of VEGF, IL1β, and TGFβ in RCF under 1% O_2, 5% O_2, and 21% O_2 culture conditions. *p<0.05, **p<0.01, ***p<0.001, ****p<0.0001

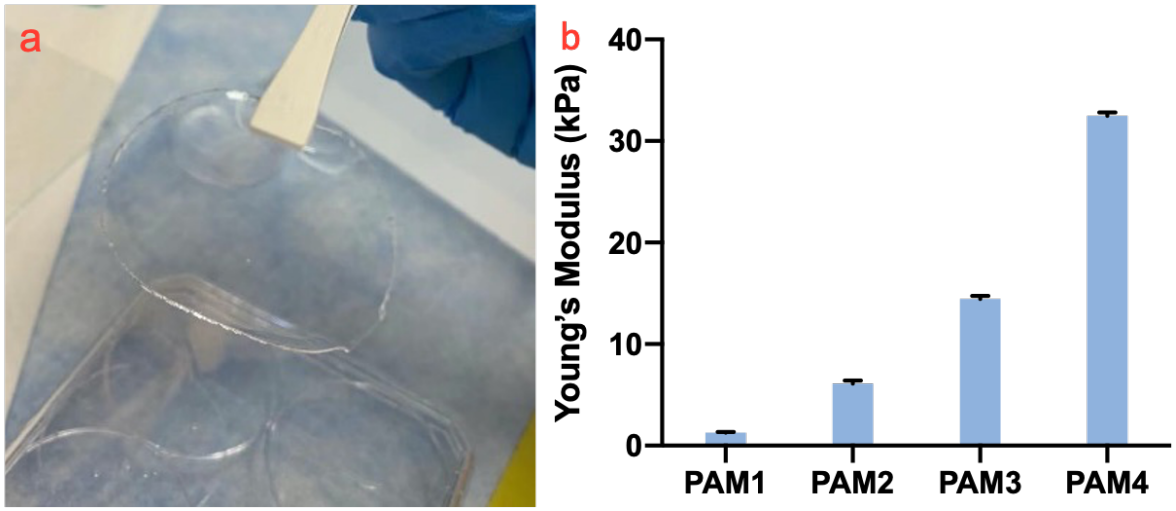

Figure 2. Fabricated PAM gel and stiffness of PAM gels as measured by rheometer.

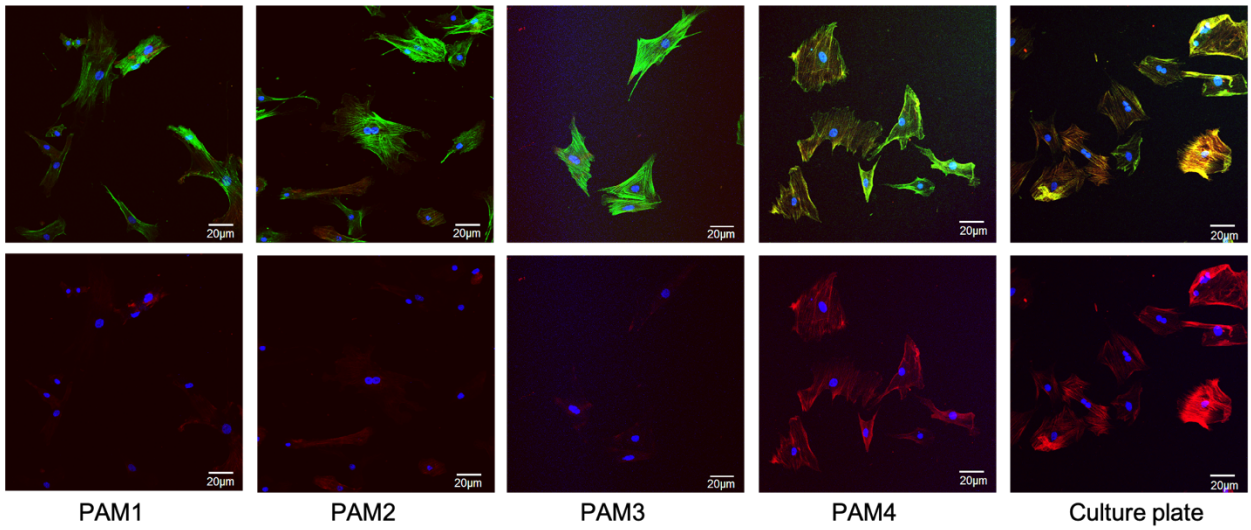

Figure 3. Immunocytochemical staining of F-actin (green) and α-SMA (red) of RCF cultured on PAM1 to 4 and culture plate. Nuclei were stained with DAPI (blue).

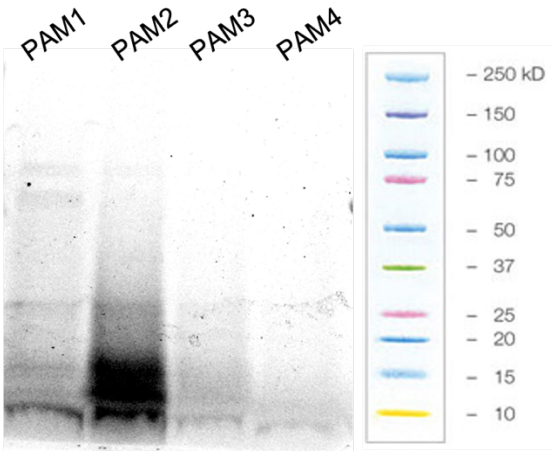

Figure 4. Protein expression of RCF cultured on PAM1 to 4 gels.

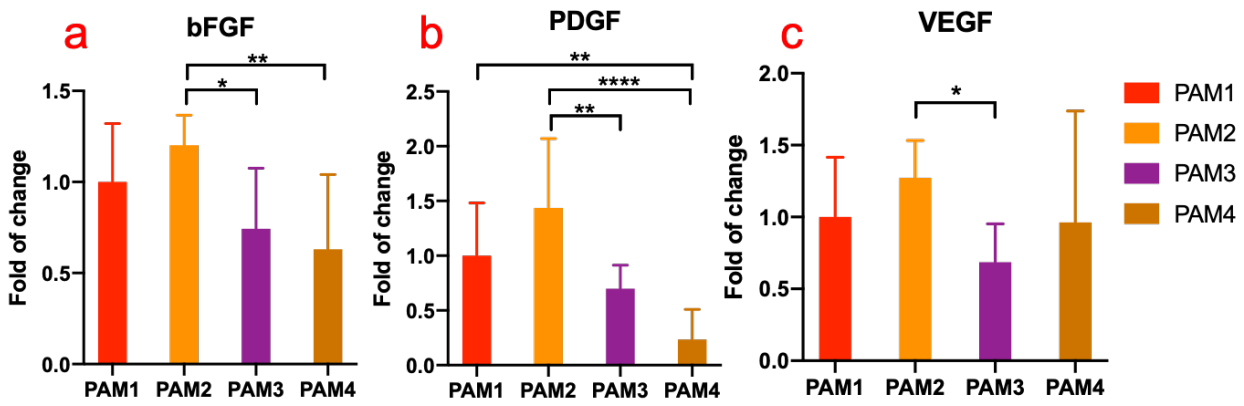

Figure 5. Gene expression of RCF cultured on PAM1 to 4. *p<0.05, **p<0.01, ***p<0.001, ****p<0.0001

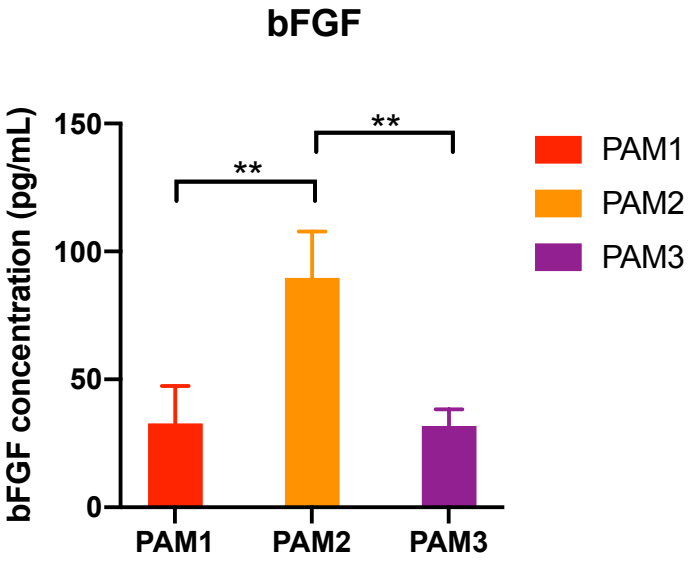

Figure 6. Concentration of bFGF of RCF secretome collected on PAM1 to 3. *p<0.05, **p<0.01, ***p<0.001, ****p<0.0001

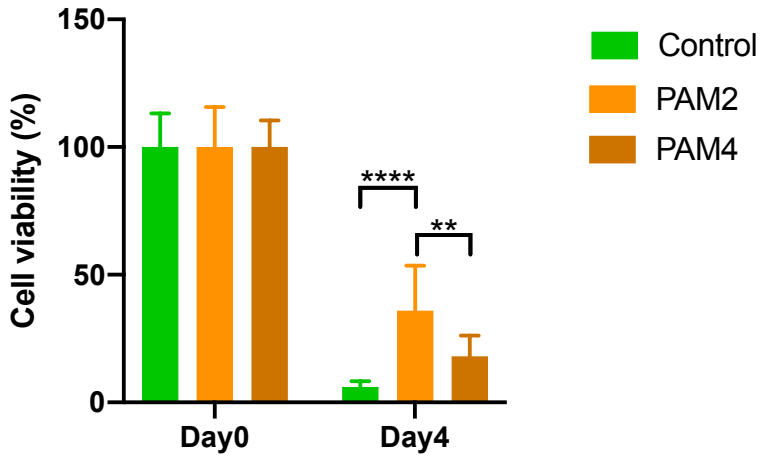

Figure 7. In vitro HUVEC survival under hypoxic condition. *p<0.05, **p<0.01, ***p<0.001, ****p<0.0001

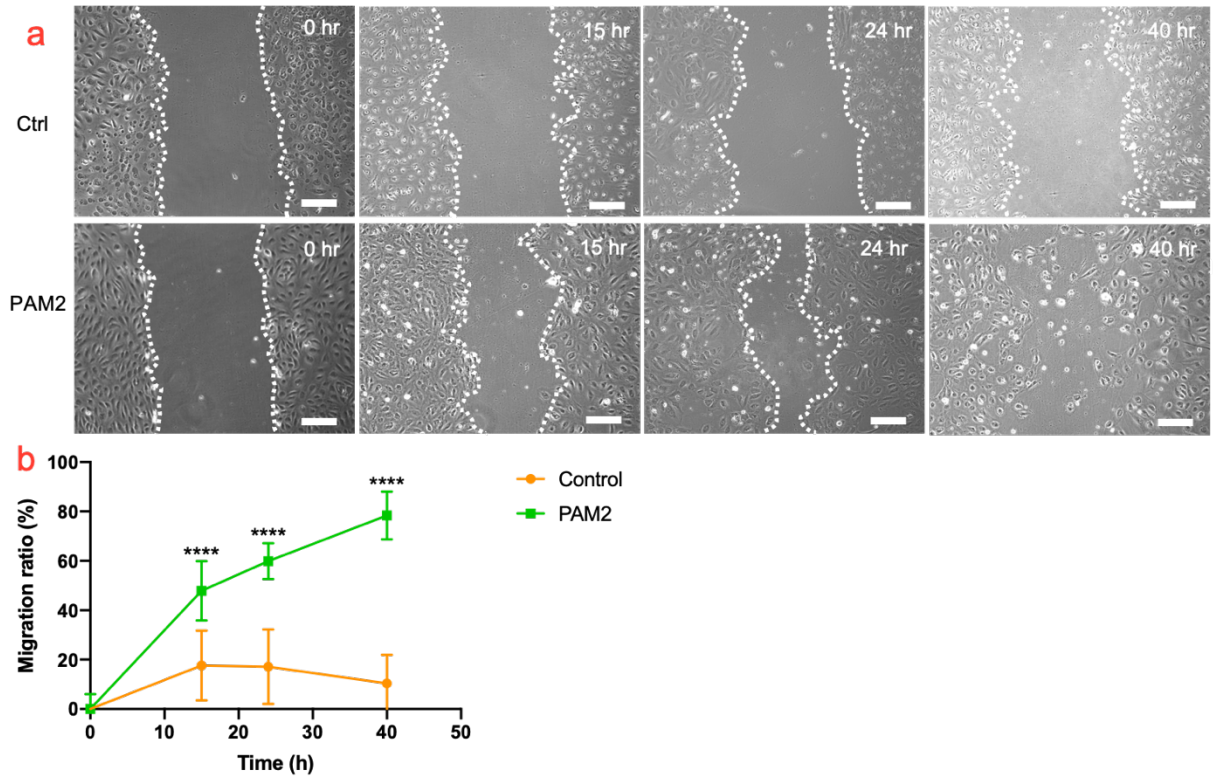

Figure 8. In vitro HUVEC migration under hypoxic condition. scale bar = 200 μm, *p<0.05, **p<0.01, ***p<0.001, ****p<0.0001

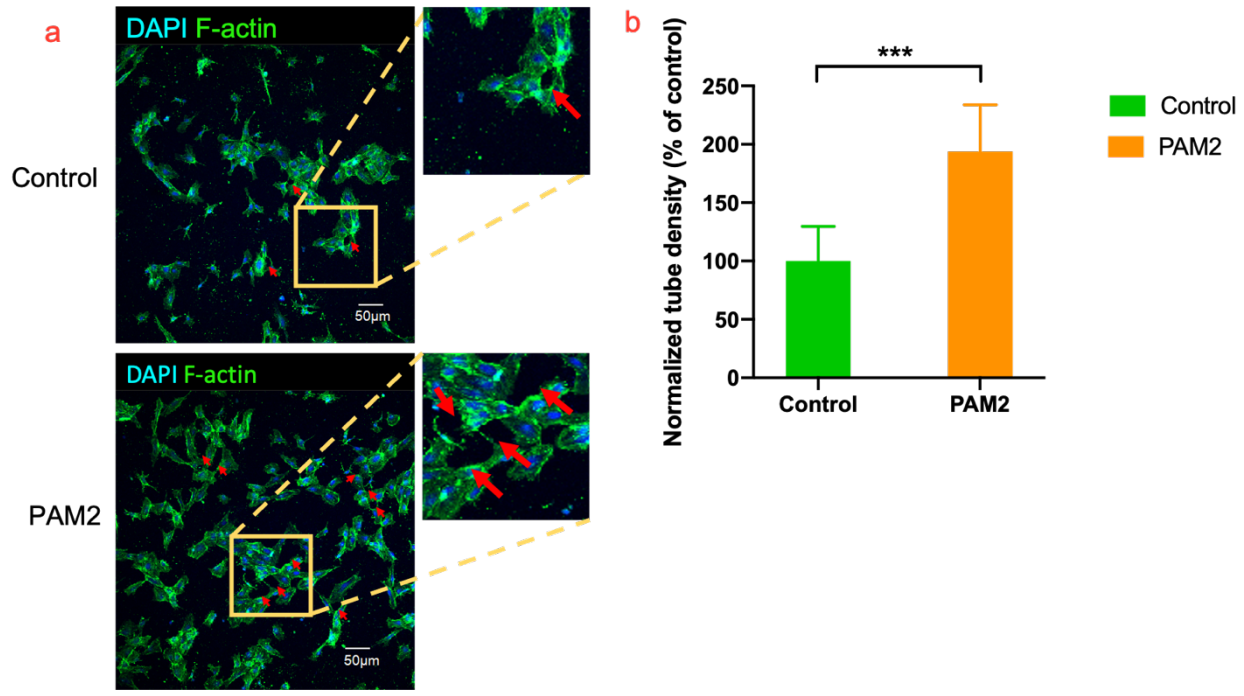

Figure 9. In vitro HUVEC tube formation under hypoxic condition with quantification. Nuclei and cytoplasm were stained with DAPI (blue) and F-actin (green). *p<0.05, **p<0.01, ***p<0.001, ****p<0.0001

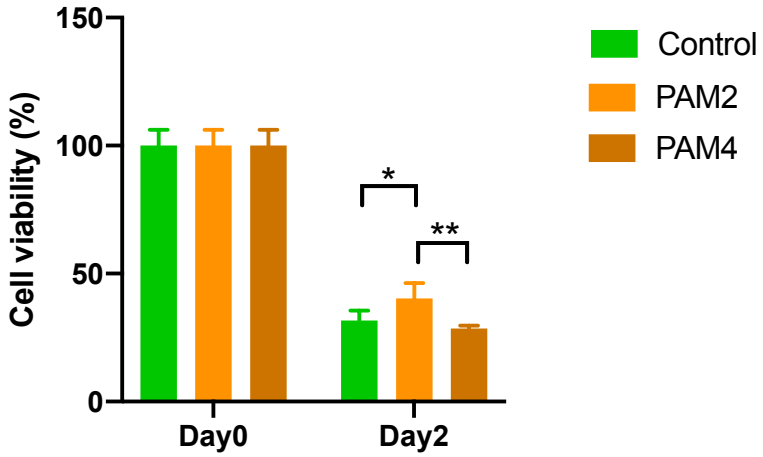

Figure 10. In vitro cardiomyocytes survival under hypoxic condition. *p<0.05, **p<0.01, ***p<0.001, ****p<0.0001

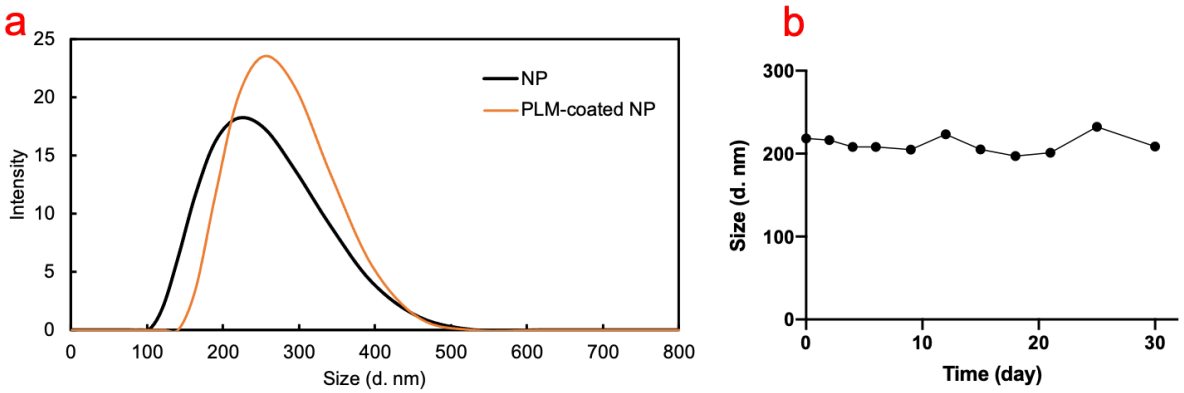

Figure 11. DLS of uncoated and PLM-coated nanoparticles and stability of uncoated nanoparticles.

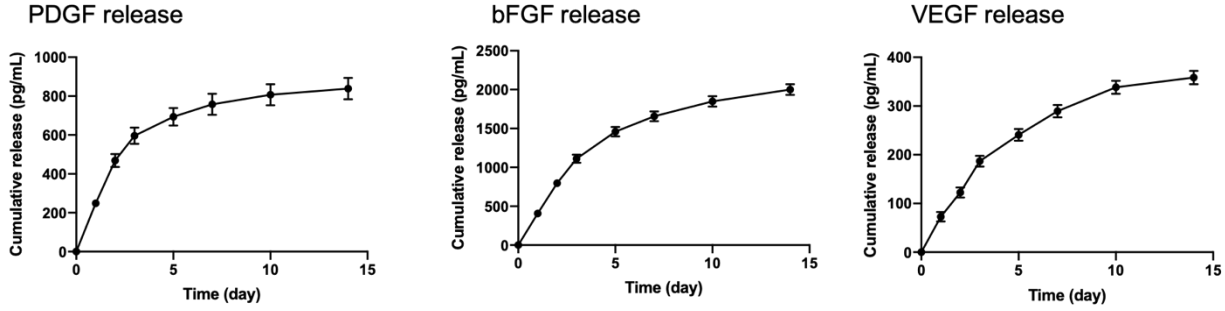

Figure 12. Growth factor release kinetics. The PDGF, bFGF, and VEGF release of the uncoated nanoparticles was tested for 14 days under 37℃.

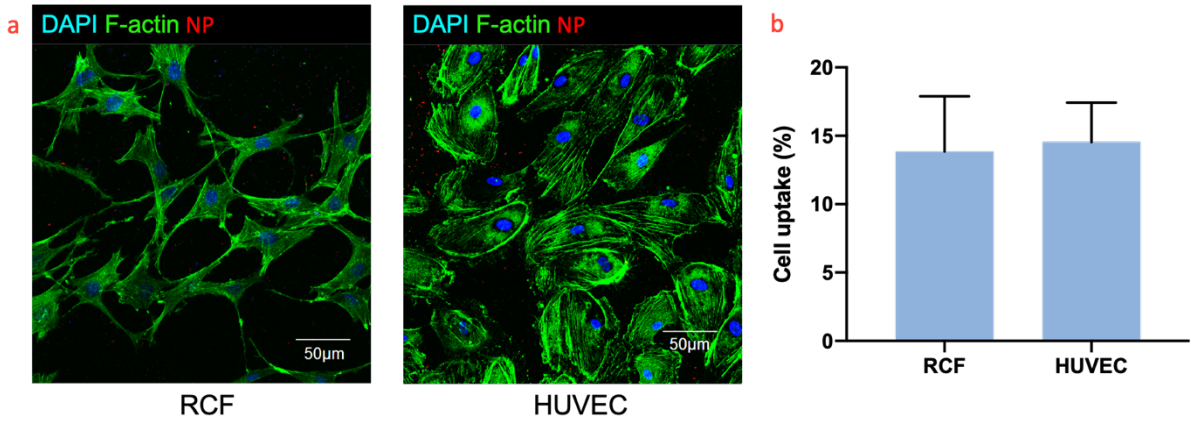

Figure 13. Cell uptake of PLM-coated nanoparticles with quantification.

Reference

1. Nascimento, B. R., Brant, L. C. C., Marino, B. C. A., Passaglia, L. G., & Ribeiro, A. L. P. (2019). Implementing myocardial infarction systems of care in low/middle-income countries. *Heart*, *105*(1), 20 LP – 26. https://doi.org/10.1136/heartjnl-2018-313398

2. Lu, L., Liu, M., Sun, R., Zheng, Y., & Zhang, P. (2015). Myocardial Infarction: Symptoms and Treatments. *Cell Biochemistry and Biophysics*, *72*(3), 865–867. https://doi.org/10.1007/s12013-015-0553-4

3. Roe, M. T., Messenger, J. C., Weintraub, W. S., Cannon, C. P., Fonarow, G. C., Dai, D., Chen, A. Y., Klein, L. W., Masoudi, F. A., McKay, C., Hewitt, K., Brindis, R. G., Peterson, E. D., & Rumsfeld, J. S. (2010). Treatments, trends, and outcomes of acute myocardial infarction and percutaneous coronary intervention. In *Journal of the American College of Cardiology* (Vol. 56, Issue 4, pp. 254–263). https://doi.org/10.1016/j.jacc.2010.05.008

4. Van de Werf, F., Bax, J., Betriu, A., Blomstrom-Lundqvist, C., Crea, F., Falk, V., Filippatos, G., Fox, K., Huber, K., Kastrati, A., Rosengren, A., Steg, P. G., Tubaro, M., Verheugt, F., Weidinger, F., & Weis, M. (2008). Management of acute myocardial infarction in patients presenting with persistent ST-segment elevation: the Task Force on the Management of ST-Segment Elevation Acute Myocardial Infarction of the European Society of Cardiology. *European Heart Journal*, *29*(23), 2909–2945. https://doi.org/10.1093/eurheartj/ehn416

5. Krishna, K. A., Krishna, K. S., Berrocal, R., Rao, K. S., & Sambasiva Rao, K. R. S. (2011). Myocardial infarction and stem cells. *Journal of Pharmacy & Bioallied Sciences*, *3*(2), 182–188. https://doi.org/10.4103/0975-7406.80761

6. Madigan, M., & Atoui, R. (2018). Therapeutic Use of Stem Cells for Myocardial Infarction.

Bioengineering (Basel, Switzerland), *5*(2). https://doi.org/10.3390/bioengineering5020028

7. Orlic, D., Hill, J. M., & Arai, A. E. (2002). Stem cells for myocardial regeneration. *Circulation Research*, *91*(12), 1092–1102. https://doi.org/10.1161/01.res.0000046045.00846.b0

8. Dhar, D., & Hsi-En Ho, J. (2009). Stem cell research policies around the world. *The Yale Journal of Biology and Medicine*, *82*(3), 113–115.

9. Ahmed, R. P. H., Ashraf, M., Buccini, S., Shujia, J., & Haider, H. K. (2011). Cardiac tumorigenic potential of induced pluripotent stem cells in an immunocompetent host with myocardial infarction. *Regenerative Medicine*, *6*(2), 171–178. https://doi.org/10.2217/rme.10.103

10. Baraniak, P. R., & McDevitt, T. C. (2010). Stem cell paracrine actions and tissue regeneration. *Regenerative Medicine*, *5*(1), 121–143. https://doi.org/10.2217/rme.09.74

11. Huang, K., Ozpinar, E. W., Su, T., Tang, J., Shen, D., Qiao, L., Hu, S., Li, Z., Liang, H., Mathews, K., Scharf, V., Freytes, D. O., & Cheng, K. (2020). An off-the-shelf artificial cardiac patch improves cardiac repair after myocardial infarction in rats and pigs. *Science Translational Medicine*, *12*(538). https://doi.org/10.1126/scitranslmed.aat9683

12. Waters, R., Alam, P., Pacelli, S., Chakravarti, A. R., Ahmed, R. P. H., & Paul, A. (2018). Stem cell-inspired secretome-rich injectable hydrogel to repair injured cardiac tissue. *Acta Biomaterialia*, *69*, 95–106. https://doi.org/10.1016/j.actbio.2017.12.025

13. Webber, M. J., Han, X., Murthy, S. N. P., Rajangam, K., Stupp, S. I., & Lomasney, J. W. (2010). Capturing the stem cell paracrine effect using heparin-presenting nanofibres to treat

cardiovascular diseases. *Journal of Tissue Engineering and Regenerative Medicine*, *4*(8), 600–610. https://doi.org/10.1002/term.273

14. Padin-Iruegas, M. E., Misao, Y., Davis, M. E., Segers, V. F. M., Esposito, G., Tokunou, T., Urbanek, K., Hosoda, T., Rota, M., Anversa, P., Leri, A., Lee, R. T., & Kajstura, J. (2009). Cardiac progenitor cells and biotinylated insulin-like growth factor-1 nanofibers improve endogenous and exogenous myocardial regeneration after infarction. *Circulation*, *120*(10), 876–887. https://doi.org/10.1161/CIRCULATIONAHA.109.852285

15. Stine, S. J., Popowski, K. D., Su, T., & Cheng, K. (2020). Exosome and Biomimetic Nanoparticle Therapies for Cardiac Regenerative Medicine. *Current Stem Cell Research & Therapy*, *15*(8), 674–684. https://doi.org/10.2174/1574888X15666200309143924

16. Oduk, Y., Zhu, W., Kannappan, R., Zhao, M., Borovjagin, A. V, Oparil, S., & Zhang, J. J. (2018). VEGF nanoparticles repair the heart after myocardial infarction. *American Journal of Physiology. Heart and Circulatory Physiology*, *314*(2), H278–H284. https://doi.org/10.1152/ajpheart.00471.2017

17. L., C. T., B., S. R., K., H. J., J., W. C., E., B. T., P., K. J., S., A. K., & A., L. L. (2020). Defining the Cardiac Fibroblast Secretome in a Fibrotic Microenvironment. *Journal of the American Heart Association*, *9*(19), e017025. https://doi.org/10.1161/JAHA.120.017025

18. Camelliti, P., Borg, T. K., & Kohl, P. (2005). Structural and functional characterisation of cardiac fibroblasts. *Cardiovascular Research*, *65*(1), 40–51. https://doi.org/10.1016/j.cardiores.2004.08.020

19. Souders, C. A., Bowers, S. L. K., & Baudino, T. A. (2009). Cardiac fibroblast: the renaissance cell. *Circulation Research*, *105*(12), 1164–1176.

https://doi.org/10.1161/CIRCRESAHA.109.209809

20. Cosme, J., Guo, H., Hadipour-Lakmehsari, S., Emili, A., & Gramolini, A. O. (2017). Hypoxia-Induced Changes in the Fibroblast Secretome, Exosome, and Whole-Cell Proteome Using Cultured, Cardiac-Derived Cells Isolated from Neonatal Mice. *Journal of Proteome Research*, *16*(8), 2836–2847. https://doi.org/10.1021/acs.jproteome.7b00144

21. Syed, S., Karadaghy, A., & Zustiak, S. (2015). Simple polyacrylamide-based multiwell stiffness assay for the study of stiffness-dependent cell responses. *Journal of Visualized Experiments : JoVE*, *97*. https://doi.org/10.3791/52643

22. Zustiak, S. P., & Leach, J. B. (2010). Hydrolytically degradable poly(ethylene glycol) hydrogel scaffolds with tunable degradation and mechanical properties. *Biomacromolecules*, *11*(5), 1348–1357. https://doi.org/10.1021/bm100137q

23. Maharaj, A. S. R., & D'Amore, P. A. (2007). Roles for VEGF in the adult. *Microvascular Research*, *74*(2–3), 100–113. https://doi.org/10.1016/j.mvr.2007.03.004

24. Szekely, Y., & Arbel, Y. (2018). A Review of Interleukin-1 in Heart Disease: Where Do We Stand Today? *Cardiology and Therapy*, *7*(1), 25–44. https://doi.org/10.1007/s40119-018-0104-3

25. Combes, A., Frye, C. S., Lemster, B. H., Brooks, S. S., Watkins, S. C., Feldman, A. M., & McTiernan, C. F. (2002). Chronic exposure to interleukin 1beta induces a delayed and reversible alteration in excitation-contraction coupling of cultured cardiomyocytes. *Pflugers Archiv : European Journal of Physiology*, *445*(2), 246–256. https://doi.org/10.1007/s00424-002-0921-y

26. Tatsumi, T., Matoba, S., Kawahara, A., Keira, N., Shiraishi, J., Akashi, K., Kobara, M., Tanaka, T., Katamura, M., Nakagawa, C., Ohta, B., Shirayama, T., Takeda, K., Asayama, J., Fliss, H., & Nakagawa, M. (2000). Cytokine-induced nitric oxide production inhibits mitochondrial energy production and impairs contractile function in rat cardiac myocytes. *Journal of the American College of Cardiology*, *35*(5), 1338–1346. https://doi.org/10.1016/s0735-1097(00)00526-x

27. Hanna, A., & Frangogiannis, N. G. (2019). The Role of the TGF-β Superfamily in Myocardial Infarction. *Frontiers in Cardiovascular Medicine*, *6*, 140. https://doi.org/10.3389/fcvm.2019.00140

28. Rao K, B., Malathi, N., Narashiman, S., & Rajan, S. T. (2014). Evaluation of myofibroblasts by expression of alpha smooth muscle actin: a marker in fibrosis, dysplasia and carcinoma. *Journal of Clinical and Diagnostic Research : JCDR*, *8*(4), ZC14-7. https://doi.org/10.7860/JCDR/2014/7820.4231

29. Turner, N. A., & Porter, K. E. (2013). Function and fate of myofibroblasts after myocardial infarction. *Fibrogenesis & Tissue Repair*, *6*(1), 5. https://doi.org/10.1186/1755-1536-6-5

30. Peterson, D. J., Ju, H., Hao, J., Panagia, M., Chapman, D. C., & Dixon, I. M. (1999). Expression of Gi-2 alpha and Gs alpha in myofibroblasts localized to the infarct scar in heart failure due to myocardial infarction. *Cardiovascular Research*, *41*(3), 575–585. https://doi.org/10.1016/s0008-6363(98)00264-8

31. van den Borne, S. W. M., Diez, J., Blankesteijn, W. M., Verjans, J., Hofstra, L., & Narula, J. (2010). Myocardial remodeling after infarction: the role of myofibroblasts. *Nature Reviews. Cardiology*, *7*(1), 30–37. https://doi.org/10.1038/nrcardio.2009.199

32. Cokkinos, D. V, & Pantos, C. (2011). Myocardial remodeling, an overview. *Heart Failure Reviews*, *16*(1), 1–4. https://doi.org/10.1007/s10741-010-9192-4

33. Ceccato, T. L., Starbuck, R. B., Hall, J. K., Walker, C. J., Brown, T. E., Killgore, J. P., Anseth, K. S., & Leinwand, L. A. (2020). Defining the Cardiac Fibroblast Secretome in a Fibrotic Microenvironment. *Journal of the American Heart Association*, *9*(19), e017025. https://doi.org/10.1161/JAHA.120.017025

34. Tong, G., Liang, Y., Xue, M., Chen, X., Wang, J., An, N., Wang, N., Chen, Y., Wang, Y., Jin, L., & Cong, W. (2020). The protective role of bFGF in myocardial infarction and hypoxia cardiomyocytes by reducing oxidative stress via Nrf2. *Biochemical and Biophysical Research Communications*, *527*(1), 15–21. https://doi.org/10.1016/j.bbrc.2020.04.053

35. Ling, L., Gu, S., Cheng, Y., & Ding, L. (2018). bFGF promotes Sca-1+ cardiac stem cell migration through activation of the PI3K/Akt pathway. *Molecular Medicine Reports*, *17*(2), 2349–2356. https://doi.org/10.3892/mmr.2017.8178

36. Yanagisawa-Miwa, A., Uchida, Y., Nakamura, F., Tomaru, T., Kido, H., Kamijo, T., Sugimoto, T., Kaji, K., Utsuyama, M., & Kurashima, C. (1992). Salvage of infarcted myocardium by angiogenic action of basic fibroblast growth factor. *Science (New York, N.Y.)*, *257*(5075), 1401–1403. https://doi.org/10.1126/science.1382313

37. Hoch, R. V, & Soriano, P. (2003). Roles of PDGF in animal development. *Development (Cambridge, England)*, *130*(20), 4769–4784. https://doi.org/10.1242/dev.00721

38. Muñoz-Chápuli, R., Quesada, A. R., & Angel Medina, M. (2004). Angiogenesis and signal transduction in endothelial cells. *Cellular and Molecular Life Sciences : CMLS*, *61*(17),

2224–2243. https://doi.org/10.1007/s00018-004-4070-7

39. Ungerleider, J. L., & Christman, K. L. (2014). Concise review: injectable biomaterials for the treatment of myocardial infarction and peripheral artery disease: translational challenges and progress. *Stem Cells Translational Medicine*, *3*(9), 1090–1099. https://doi.org/10.5966/sctm.2014-0049

40. Ferrari, R., Sponchioni, M., Morbidelli, M., & Moscatelli, D. (2018). Polymer nanoparticles for the intravenous delivery of anticancer drugs: the checkpoints on the road from the synthesis to clinical translation. *Nanoscale*, *10*(48), 22701–22719. https://doi.org/10.1039/C8NR05933K

41. Hu, C.-M. J., Fang, R. H., Wang, K.-C., Luk, B. T., Thamphiwatana, S., Dehaini, D., Nguyen, P., Angsantikul, P., Wen, C. H., Kroll, A. V, Carpenter, C., Ramesh, M., Qu, V., Patel, S. H., Zhu, J., Shi, W., Hofman, F. M., Chen, T. C., Gao, W., … Zhang, L. (2015). Nanoparticle biointerfacing by platelet membrane cloaking. *Nature*, *526*(7571), 118–121. https://doi.org/10.1038/nature15373

42. Tang, J., Su, T., Huang, K., Dinh, P.-U., Wang, Z., Vandergriff, A., Hensley, M. T., Cores, J., Allen, T., Li, T., Sproul, E., Mihalko, E., Lobo, L. J., Ruterbories, L., Lynch, A., Brown, A., Caranasos, T. G., Shen, D., Stouffer, G. A., … Cheng, K. (2018). Targeted repair of heart injury by stem cells fused with platelet nanovesicles. *Nature Biomedical Engineering*, *2*, 17–26. https://doi.org/10.1038/s41551-017-0182-x

43. Fan, Z., Xu, Z., Niu, H., Sui, Y., Li, H., Ma, J., & Guan, J. (2019). Spatiotemporal delivery of basic fibroblast growth factor to directly and simultaneously attenuate cardiac fibrosis and promote cardiac tissue vascularization following myocardial infarction. *Journal of*

Controlled Release : Official Journal of the Controlled Release Society, *311–312*, 233–244. https://doi.org/10.1016/j.jconrel.2019.09.005

44. Xu, Y., Fu, M., Li, Z., Fan, Z., Li, X., Liu, Y., Anderson, P. M., Xie, X., Liu, Z., & Guan, J. (2016). A prosurvival and proangiogenic stem cell delivery system to promote ischemic limb regeneration. *Acta Biomaterialia*, *31*, 99–113. https://doi.org/10.1016/j.actbio.2015.12.021

45. Alasvand, N., Urbanska, A. M., Rahmati, M., Saeidifar, M., Gungor-Ozkerim, P. S., Sefat, F., Rajadas, J., & Mozafari, M. (2017). *Chapter 13 - Therapeutic Nanoparticles for Targeted Delivery of Anticancer Drugs* (A. M. B. T.-M. S. for C. D. Grumezescu Biosensing and Diagnostics (ed.); pp. 245–259). Elsevier. https://doi.org/https://doi.org/10.1016/B978-0-323-52725-5.00013-7